Composite Structures 190 (2018) 169–178

Contents lists available at ScienceDirect

Composite Structures

journal homepage: www.elsevier.com/locate/compstruct

# Analysis of DCB test of angle-ply laminates including bending-twisting coupling

J. De Gracia[a,*], A. Boyano[a], A. Arrese[b], F. Mujika[b], Materials + Technologies Group/Mechanics of Materials

[a] Department of Mechanical Engineering, Faculty of Engineering of Vitoria-Gasteiz, University of the Basque Country (UPV/EHU), Nieves Cano, 12, 01006 Vitoria-Gasteiz, Spain
[b] Department of Mechanical Engineering, Faculty of Engineering of Gipuzkoa, University of the Basque Country (UPV/EHU), Plaza de Europa, 1, 20018 San Sebastián, Spain

ARTICLE INFO

*Keywords:*
Delamination
Double Cantilever Beam
Multidirectional
Coupling effects

ABSTRACT

Interlaminar fracture of angle-ply symmetric and anti-symmetric laminates by means of the Double Cantilever Beam test has been analyzed. As the cracked arms are symmetric in both cases, bending-twisting coupling occurs. Nevertheless, the effect of that coupling is different in symmetric and anti-symmetric cases. In symmetric cases, it induces a non-uniform aperture of the arms associated to mode I. In anti-symmetric cases, the effect is a sliding of both arms associated to mode III. The analytic approach of the energy release rate includes those coupling effects. Besides the present approach, experimental results are reduced with a previous approach that does not include coupling effects and with the area method.

## 1. Introduction

One of the most common damage mechanism in laminated composites is delamination, due to the low interlaminar strength of these materials. According to linear elastic fracture mechanics (LEFM) there are three modes of fracture, mode I or opening mode, mode II or sliding mode and mode III or tearing mode [1].

The Double Cantilever Beam (DCB) test is widely used for the determination of interlaminar fracture toughness in mode I. The LEFM principles are applied and used to measure the energy dissipated per unit area of crack growth, known as the energy release rate $G_I$, of unidirectional laminates. The test has been standardized for carbon fiber reinforced plastic (CFRP) specimens [2,3]. Despite the fact that the test is very simple, it requires the optical determination of the growing interlaminar crack. Nevertheless, sometimes the crack tip is difficult to observe and it can prevent from obtaining a good characterization of the material. Some authors have dealt with this issue by means of different methods. Szekrényes uses a transparent material in order to identify the crack front [4]. Yoshihara and Kawamura [5] obtained compliance independently from the crack length using the longitudinal strain of the top surface of the specimen. De Moura et al. [6] proposed a method, based on a crack equivalent concept, to consider the fracture process zone at the crack tip. De Gracia et al. [7] proposed a method to determine the crack length by means of the change on the specimen compliance during the test.

In spite of standards have been developed for DCB unidirectional specimens, this test configuration has been also used to calculate $G_{Ic}$ of multidirectional laminates [8–10]. Choi et al. [11] and Morais [12] have assessed the applicability of the test for those laminates, determining that it can be valid if deviations of the delamination from the central plane are avoided. Factors which may affect seriously the test in the case of multidirectional specimens are laminate lay-up, symmetry of the laminate, curved crack front, mode mixture, residual stresses or damage during the crack growth (fiber bridging effect, fiber matrix debonding, or fiber breakage) [13]. An appropriate selection of the stacking sequence may prevent those issues, making their effect on $G_{Ic}$ negligible and leading to a nearly pure mode I [12]. Nevertheless, this is not always possible since the industry uses laminates with a wide range of sequences and therefore couplings and residual stresses are often present. Taking all these factors into account, in addition to the fact that initiation value is the most conservative toughness value, delamination toughness from the DCB test on multidirectional laminates should probably be quantified just for initiation values.

Extensive research concerning mode I has been led to develop analytical solutions for DCB specimens. The elastic foundation was first applied by Kanninen [14] for the DCB specimen to model the deflection and rotation at the crack tip zone improving the application of the simple beam theory. Williams [15] extended Kanninen's model for

* Corresponding author.
*E-mail address:* juan.degracia@ehu.eus (J. De Gracia).

https://doi.org/10.1016/j.compstruct.2018.02.021
Received 25 October 2017; Received in revised form 2 February 2018; Accepted 12 February 2018
Available online 13 February 2018

**Nomenclature**

| | |
|---|---|
| $a$ | delamination length ($mm$) |
| $[a]$,$[b]$,$[c]$ | compliance matrices |
| $a_{mn}$ | in-plane compliance coefficients ($mm/N$) |
| $b$ | DCB specimen width ($mm$) |
| $d_{mn}$ | flexural compliance coefficients $(N{\cdot}mm)^{-1}$ |
| $\{e\}_k$ | hygrothermal strain matrix at lamina$k$ |
| $F_1$,$F_2$,$F_3$ | equivalent point forces for distributed load ($N$) |
| $G_I$,$G_{II}$,$G_{III}$ | strain energy release rate in mode I, II, III ($J/m^2$) |
| $G_C$ | critical strain energy release rate ($J/m^2$) |
| $h$ | thickness of the cracked arm ($mm$) |
| $L$ | length of the specimen ($mm$) |
| $\{\overline{M}\}$ | matrix of the sum of mechanical and hygrothermal moments |
| $M_i$ | bending moment per unit length at section $i$ ($N$) |
| $M_{s_i}$ | twisting moment per unit length at section $i$ ($N$) |
| $m_i$ | bending moment at section $i$ ($N{\cdot}mm$) |
| $m_{t_i}$ | twisting moment at section $i$ ($N{\cdot}mm$) |
| $\{\overline{N}\}$ | matrix of the sum of mechanical and hygrothermal forces |
| $N_x^{HT}$,$N_y^{HT}$ | hygrothermal forces per unit length ($N/mm$) |
| $P$ | opening load on the DCB specimen ($N$) |
| $[Q]_k$ | reduced stiffness matrix at lamina$k$ |
| $q_{10}$,$q_{30}$ | maximum intensities of the distributed forces in the model ($N/m$) |
| $S_{ij}$ | compliance coefficients of lamina$k$ |
| $U^*$ | complementary strain energy ($N/m$) |
| $u$,$v$,$w$ | displacement components |
| $u_0$,$v_0$,$w_0$ | displacement components in the middle plane |
| $V_q$,$V_r$ | out-of-plane shear stress resultants |
| $x_1$,$x_2$,$x_3$ | parameters of the distributed forces ($mm$) |
| $z_k$ | distance from the mid-plane to the lower surface of the $k^{th}$layer. |
| $\alpha_0$,$\alpha_1$,$\alpha$ | parameters depending on$x_1$,$x_2$,$x_3$ |
| $\gamma_{xy} = \gamma_s$ | in-plane shear strain |
| $\gamma_{yz} = \gamma_q$,$\gamma_{zx} = \gamma_r$ | out-of-plane shear strains |
| $\delta_i$ | generalized displacement at point $i$ in the direction of$F_i$ |
| $\varepsilon_x$,$\varepsilon_y$,$\varepsilon_z$ | normal strains |
| $\varepsilon_x^0$,$\varepsilon_y^0$ | normal strains in the middle surface |
| $\theta_x$ | bending angle |
| $\theta_y$ | twisting angle |
| $\kappa_x$,$\kappa_y$ | bending curvatures of the middle surface |
| $\kappa_s$ | twisting curvature of the middle surface |
| $\{\sigma\}_k$ | in plane stress matrix at lamina$k$ |

orthotropic materials, while Ozdil and Carlsson [16] extended it to angle-ply laminates taking into account out-of-plane stiffness. Szekrényes [17] presented an improved analysis including Winkler–Pasternak foundation, transverse shear, Saint–Venant effect and crack tip shear deformation. Olsson [18] reviewed these and posterior works [19,16,20] concerning beams on elastic foundation, concluding that the use of energy approaches to incorporate the crack tip compliance or Timoshenko beams on a Winkler foundation are the methods that best fit to FEM results. Other methods to obtain an analytical solution involve beam theory and the specimen compliance [7] or include a rotational spring to a clamped beam [21,22].

The previous models regarding interlaminar toughness in multidirectional laminates are mainly applied to stacking sequences that avoid bending-twisting coupling. However, twisting curvatures and residual stresses due to hygrothermal effects can appear when other sequences are used. Concerning these effects, a new analytical approach has been recently proposed [23]. The model presented leads to calculate the total energy release rate in the DCB test including the contribution residual stresses to the energy release rate. In the mentioned work, the semi-laminates or cracked arms of the specimen were antisymmetric and thus there was not bending-twisting coupling in each arm. Moreover, the distribution of the twisting moment per unit length across the width was assumed to be uniform.

The main goal of the present study is to include the effect of the bending-twisting coupling in the analysis of the DCB test. The sequences studied are $[(\pm45/\pm45)_s]_s$ symmetric and $[(\pm45/\pm45)_s]_{as}$ antisymmetric. The properties of the symmetric cracked arms are the same in both cases, but the orientation of the plies that form the interlaminar crack is different, (+45/+45) in the first case and (+45/−45) in the second one.

As the arms of the specimens studied are symmetric, the existence of bending-twisting coupling provokes a rotation in each cracked arm induced by the bending moment applied by means of piano hinges or load blocks. In the case of anti-symmetric laminates both arms rotate in the same sense, whereas if the laminate is symmetric the rotations are opposite, as shown in Fig. 1. Then, there is a rigid body rotation of the non-cracked part in the case of anti-symmetric specimens. In the case of symmetric laminates there is a non-uniform load distribution applied to the piano hinges, whose resultant and resultant moment are the applied force $P$ and an unknown twisting moment $m_t$, respectively, preventing the rigid body rotation of the non-cracked part.

The distribution of the twisting moment per unit length across the width has been considered not uniform in the analysis of the contribution of the bending-twisting coupling to the energy.

## 2. Analytical approach

### 2.1. Displacement and strain fields

In order to model the specimens used in this work a strip type geometry is assumed. Fig. 2 shows the reference system used in the present analysis, where the plane $xy$ is equidistant from the upper and lower surfaces of the laminate. The displacement field is assumed to be given by:

$$\begin{aligned} u(x,y,z) &= u_0(x,y) + z\theta_x(x,y)\\ v(x,y,z) &= v_0(x,y) + z\theta_y(x)\\ w(x,y) &= w_0(x) - y\theta_y(x) \end{aligned} \quad (1)$$

where $u$, $v$ and $w$ are the displacements in $x$, $y$ and $z$ directions, respectively. $u_0$, $v_0$ are the displacements of the middle plane, where $z = 0$ and $w_0$ is the bending displacement of the middle line, where $y = z = 0$. $\theta_x$ is the bending angle and $\theta_y$ is the twisting angle. Fig. 3 includes the geometry of deformation in the $yz$ and $xz$ planes, showing that $\theta_y$ depends only on $x$ coordinate. Then, the whole section of the specimen rotates as a rigid body according to this angle. In the case of $\theta_x$, it is assumed that also varies with $y$ coordinate and thus the straight line AC shown in Fig. 3 varies with respect to $y$. Therefore, the cross sections do not remain plane but they become a ruled surface. Strains associated to this field can be found from Eq. (1), resulting in:

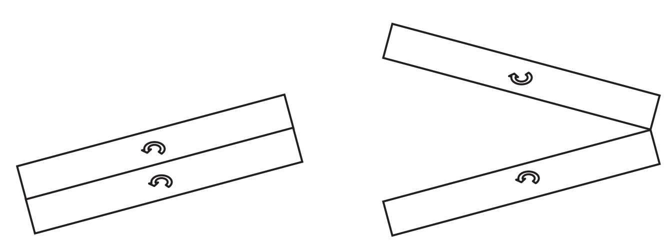

**Fig. 1.** Rotations at the crack tip. a) Anti-symmetric laminate b) Symmetric laminate.